

X. Bourrat, Pyrocarbon performances and characterization, *Proceed. Carbon'09, World Conf on Carbon, Biarritz June 14-19, 2009, T11, ID 792.*

Pyrocarbon performances and characterization

Xavier Bourrat

Orleans University - CNRS, ISTO 1A rue de Férollerie, 45071 Orléans Cedex 2, France

E-mail : Xavier.Bourrat@univ-orleans.fr xbourrat@gmail.com

Abstract. Pyrocarbon is a key material in the field of C/C composites, for aircraft brake disks, exit cones and nozzles for rocket motors or nose shields for strategic missiles. This abstract published elsewhere [1] provides a comprehensive survey on pyrocarbon properties and characterization, say: transmission electron microscopy, optical microscopy and Raman spectroscopy.

1. Introduction


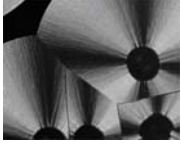
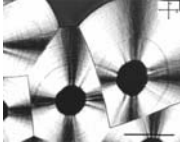
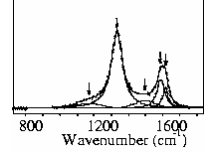
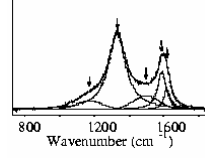
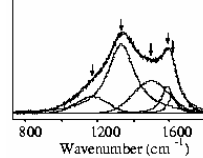
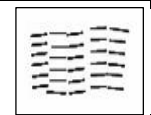

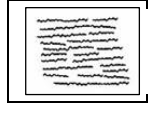
Pyrocarbons belong to a family of carbon materials that contains at least 95% of carbon and up to 5% of hydrogen [2]. They are deposited following various chemical vapour-based mechanisms [3]. Process controls structure, density as well as many other properties, like heat conductivities, elastic modulus, toughness, *etc...* For example density goes from 1 to 2.2. Some of the pyrocarbons properties are summarized in Table 1.

The development of a new process named Pulse-CVI (for chemical vapour infiltration with pulsed pressure) was a key for the recent progresses in the fundamental understanding of CVI processes [5] (say chemical vapour deposition and infiltration, respectively). Pulse-CVI was particularly interesting for controlling t_R - the residence time and gas phase maturation – a key parameter to understand CVI. The main success was the discovery of a new pyrocarbon structure deposited with a long residence time t_R and thereafter a high gas phase maturation. This is a graphitizable pyrocarbon first patented [6] and then called ‘Regenerative laminar Pyrocarbon’ in the open literature [7]. Part 1 shows that this anisotropic pyrocarbon is as dense as Rough Laminar Pyrocarbon but its lattice defects are different : it is the key control for in-service performances [1]. The multiscale structure characterization is critical as shown in the following parts.

2. “Regenerative Laminar Pyrocarbon”: a new grade of graphitizable pyrocarbon

Regenerative Laminar is very anisotropic and graphitizable [7]. Its anisotropy is as high as that of Rough laminar. Meanwhile, its lattice is seen to possess a high amount of defects. Diffraction gives a pattern of “amorphous-like” carbon but highly anisotropic. The presence of these defects is perfectly measured by the broadening of the Raman D-band : high $FWHM_D$ (see Table 1 and part 4).

Table 1. Regenerative Laminar pyrocarbon, compared to the well known Rough and Smooth Laminars [19].

	Rough laminar (RL)	Smooth laminar (SL)	Regenerative laminar (ReL)
Optical Microscopy (cross polarized light) (bare is 10µm)			
Raman (1st order) Increasing bands broadening			
d (g.cm ⁻³)	2,13	1,95	2,11
H (mass%)	4,4%	2,3%	3,5%
OA _{0.1} TEM anisotropy (0.1µm selected area)	25°	65°	34°
Ae optical anisotropy	22°	12°	22°
R _{max} Maximum reflectance	26,6%	-	32%
R _{min} Minimum reflectance	8%	-	9%
TEM Lattice organisation			

Regenerative Laminar forms following a homogeneous growth mechanism. Residence time is long. Gaseous phase produces large PAH molecules (Polycyclic Aromatic Hydrocarbons) which deposit by physisorption on the growth surface [8]. The low diffusivity and reactivity of these molecules on the surface limit the perfection of the lattice, trapping a high amount of defects and hydrogen.

3. Anisotropy : quantitative assessment by TEM

Pyrocarbon has a multiscale structure. At short range, was developed a quantitative computer application (AnaDif) based on electron diffraction pattern image analysis. AnaDif gives what is call the “orientation angle” OA [9] of the electron diffraction arcs of the pyrocarbon : 20° (strong anisotropy) < OA < 90° (weak anisotropy). The interest of this method is straightforward. It gives the scale function of the pyrocarbon, just by changing the selected area that diffracts from ~ 0.1µm

to 2 μ m. Table 2 illustrates the power of this approach. Rough Laminar OA value depends on the opening of the selected area aperture : at the scale of 100nm the angle is 25° meaning a high anisotropy. At long range it increases up to 35°: the anisotropy decreases. In the case of Regenerative Laminar the anisotropy is not so high locally but keeps constant in-between 0.1 to 2.15. This is due to the presence of the regenerative cones during the growth process of the so called Regenerative Laminar pyrocarbon.

Table 2. OA Anisotropy of Rough and Regenerative Laminars (RL and ReL, respectively), as a function of the range selected (TEM diffraction selected area) [7].

	Selected area (aperture diameter, μ m)			
	0.11	0.4	0.8	2.15
OA measured in ReL	34°	32°	32°	35°
OA measured in RL	25°	35°	35°	37°

4. Optical properties of pyrocarbons

An abundant literature is available on this subject. Optical methods have long been the best means to achieve the measurement of carbon anisotropy [10-11]. We first introduced Ae the so called Extinction Angle technique in 1995 [12] to distinguish the different laminar families from 4° to approx. 20° or 22° depending on the source wavelength. Then, Bourrat *et al.*, 2000 cross-check Ae with OA in 2000 [9]. Finally, in a recent paper we detailed the optical properties of pyrocarbons and demonstrated the physical accuracy of this technique [4].

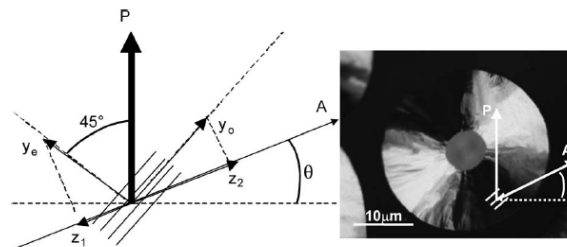
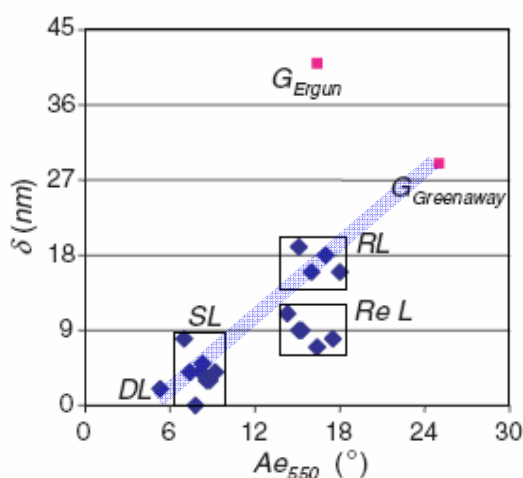


Figure 1. Extinction Angle basics. The incident polarized wave P is reflected in two waves along the two main directions of graphite. These two waves will interfere onto the plane of the analyzer, rotated by an angle $\theta = Ae$ from its crossed position, the quadrant extinguishes [4].

Ae, the extinction angle can be measured on any optical microscope equipped with a rotating analyzer. An example is given in Fig. 1. When the two Nicols are crossed, a Maltese cross appears inside the pyrocarbon coating around the fiber. Rotating the analyzer anticlockwise (θ angle), the quadrant extinguishes and then becomes bright again. The angle value for the maximum extinction is called the extinction angle Ae and is expressed in degree.

With this technique Rough and Regenerative Laminars have the same value : $A_e > 18^\circ$. Before the discovery of Regenerative Laminar, all the papers in the literature (our group and others) have systematically called any pyrocarbon with a high A_e value 'Rough Laminar'. Many papers have to be revisited with this new vision.

In our last paper we used a spectrophotometer to validate a calculated model of optical properties. The optical phase shifts as well as the ordinary and extraordinary reflectance were obtained by fitting the experimental data to the theoretical model. The extinction angle A_e and phase shift are proposed to distinguish the various families of pyrocarbons. As shown on Fig. 2 the optical properties allow to clearly distinguishing the different pyrocarbons. Regenerated Laminar pyrocarbons exhibit a lower phase shift as compared to Rough Laminar. This behavior is in line with the many defects observed in the LRe lattice by TEM or Raman spectroscopy (see next Part).



energy $E_L < 3$ eV can be successfully correlated with the phonon dispersion curves, covering a large area of the 2D graphite Brillouin zone [18].

The width of the Raman D band ($FWHM_D$) is very sensitive to low energy structural defects (e.g., disorientation of the graphene layers). For a long time, the D-band has been empirically connected to defects. The role of the defects in the broadening of the D-band is now well understood, thanks to the 'double resonance' theory. On that basis we have proposed to quantify the graphene defects by measuring the D-band broadening, corresponding to the LO phonon [19]. The D-band was preferred because it is easily subtracted: its full width at half maximum ($FWHM_D$) is inversely proportional to the life time of the phonon : the higher the defects density, the shorter the phonon's life time and the larger the $FWHM_D$.

First the Raman parameter ' $FWHM_D$ ' was calibrated during graphitization. The large difference observed among pristine pyrocarbons disappears by a treatment below 1600°C as shown on Fig. 3. Then $FWHM_D$ subsequently decreases linearly up to 2000° C and remains almost constant beyond this temperature. These structural defects, healed to a large extent after a heat treatment at 2000° C, were assumed to be in-plane local disorientation or dislocation by Rouzaud *et al.* [20] in their study of pyrolytic carbon films.

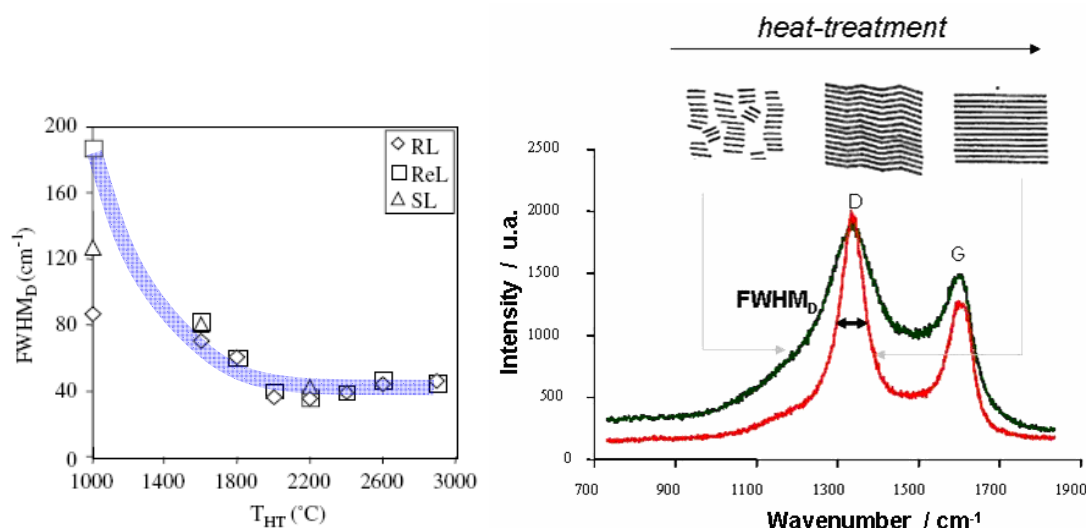


Figure 3. Sharpening of the D band ($FWHM_D$) versus heat treatment temperature for the 3 main pyrocarbons (right: schematic showing the sharpening of the peak with heat treatment) [19].

This two-stage structural improvement is accurately monitored by means of L_a , the in-plane coherence length determined by XRD. The two main stages of the graphitization process can be evidenced in Fig. 4, as the heat treatment temperature increases. The first stage is characterized by a large decrease of $FWHM_D$ up to 2000° C and corresponds to the gradual straightening of the graphene planes. The second stage ($T_{HT} > 2000$ ° C) is defined by the lateral extension of the layers and results in the increase of L_a (Fig. 4), while $FWHM_D$ remains almost equivalent for all the pyrocarbons. The latter parameter therefore appears as a very reliable indication of the heat treatment temperature encountered by pyrocarbons (at

least below $THT = 2000^\circ C$). The *sensitivity of $FWHM_D$ to the in-plane defects makes this parameter particularly relevant for the structural characterization of as-deposited pyrocarbons.*

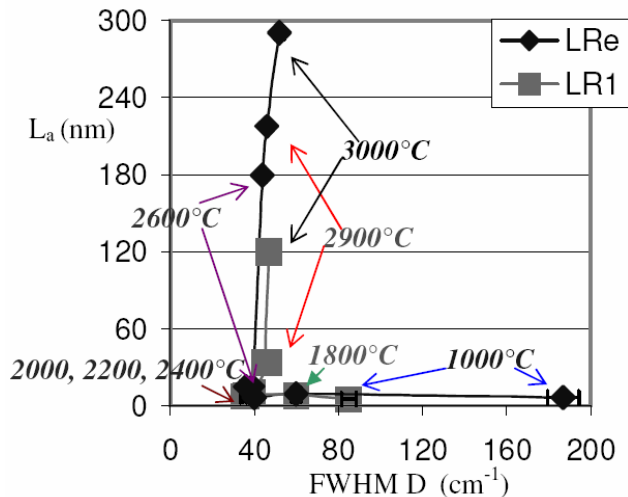
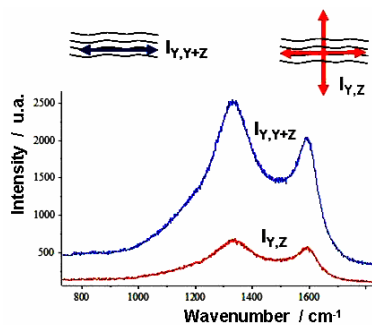


Figure 4. $FWHM_D$ of the Regenerative Laminar (LRe) and Rough Laminar (LR1 for LR number 1) pyrocarbons as a function of L_a and the heat treatment temperature [19].

6 Discussion : pyrocarbon structural classification based on polarized Raman spectroscopy

Pyrocarbon has a multiscale structure. That is why classification attempts based exclusively on anisotropy have failed in the past. It is necessary to associate a lattice criterion to the anisotropy in order to complete the structural description. Raman D-band broadening, $FWHM_D$, is the ideal structural parameter. X-ray or TEM parameters are efficient but difficult to measure in routine.



$$R_A = \frac{\int_{800}^{1850} I_{Y,Y+Z} \cdot d\nu}{\int_{800}^{1850} I_{Y,Z} \cdot d\nu}$$

Figure 5. Polarized Raman spectroscopy. The ratio of the intensity measured with the polarizer alone (blue curve) on the intensity

measured with an analyzer in cross position (red curve) gives R_A : the Raman anisotropy factor [19].

As for the anisotropy, A_e or O_A can be used but we decided to develop a measurement of the anisotropy directly on the Raman microscope. We called it R_A , the **Raman anisotropy factor**. Both G and D bands correspond to the same phonon LO and are polarized, parallel to the graphene planes. The Raman scattered beam is itself polarized parallel to the graphene planes. If an analyzer is introduced in a crossed position regarding the polarized direction of the incident beam, it is possible to measure the scattering intensity of the disoriented planes.

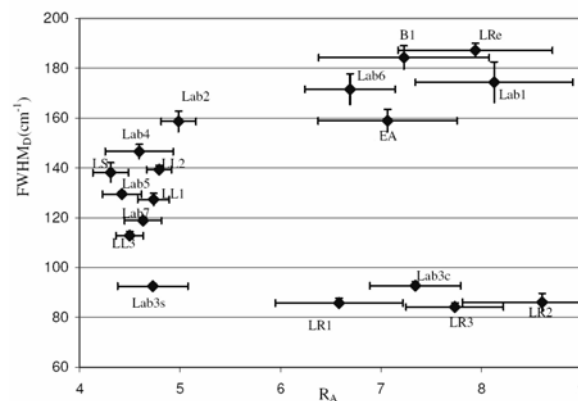


Figure 6. Plot of $FWHM_D$ versus R_A , of all the pyrocarbons available from the different processes [19].

Our technique is very simple as shown in Fig. 5. Signals are weak but accurate enough to be used: R_A is the ratio of the Raman intensity (800 to 1850 cm^{-1}) measured without analyzer on that with the analyser. Experimentally, R_A varies from 2.2 for the isotropic pyrocarbon up to more than 8 for the highest anisotropic ones.

The plot of the 18 samples processed with all the techniques available is shown in Fig. 6. Pyrocarbons with the lowest anisotropy scatter parallel to the ordinate. On the contrary, pyrocarbons with the highest anisotropy are divided into two classes : those with a high amount of defects on the top and those with a low content on the back. These 3 populations correspond to the 3 mechanisms observed by the kinetics approach [21]. The interpretation of this result is summarized in Fig. 7.

Each of the three growth mechanisms known so far, occupies one specific area in this diagram. Following the arrow which characterizes the increasing maturation of the gas phase, it is successively obtained : Rough Laminar pyrocarbon with an heterogeneous mechanism at very short residence time, Dark Laminar with a 2^d heterogeneous mechanism and the homogeneous Regenerative Laminar for long residence time. Smooth Laminar (SL) and Granular (G) are intermediate structures. An example of the *in situ* transition characterization is given in the next part.

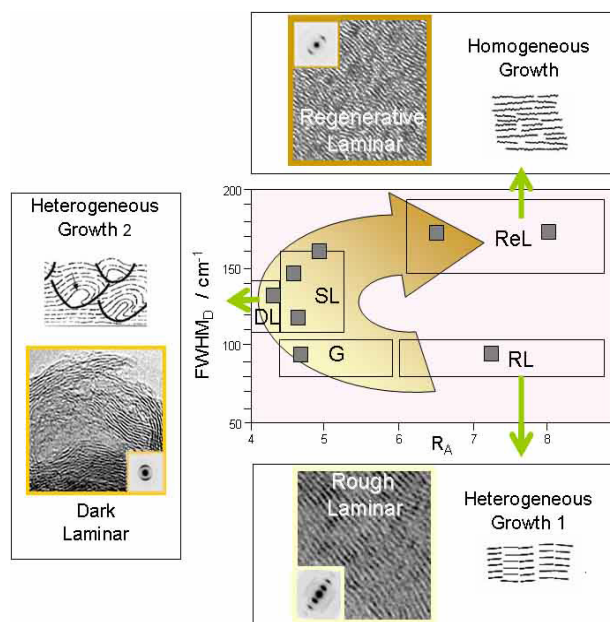


Figure 7. The three main pyrocarbon-growth-mechanisms in the $FWHM_D$ vs R_A diagram : RL, rough lamellar; ReL, regenerative lamellar and D, dark lamellar (G, granular and SL, smooth lamellar are considered as intermediates). Each structure is illustrated with its HR-TEM image in high resolution and electron diffraction [1].

7. Conclusions

These techniques were successfully applied in different fields where carbon structure is critical, for example:

- protection against the oxidation of reinforced-carbon composites [22]
- control of the interface in carbon-reinforced composites [23-26]
- pyrocarbon as a confinement barrier for nuclear reactor fuel particles [27-30].

Acknowledgments

The “Conseil Régional d’Aquitaine” is acknowledged for the different grants all along this project. I would like to associate all the students who have participated to this project: Cédric Descamps, Pascal Dupel, Olivier Féron, Damien Feuillu, Arnaud Fillion, Jérôme Lavenac, Hélène Le Poche, Arnaud Mouchon, Nicolas Reuge, Béatrice Trouvat and Jean-Marie Vallerot.

Literature cited

- [1] X. Bourrat, F. Langlais, G. Chollon and G. L. Vignoles Low Temperature Pyrocarbons : a review, *J. Braz. Chem. Soc.*, 2006 ;17:1090-5 http://jbcs.sbq.org.br/online/2006/vol17_n6/04-06147RV.pdf
- [2] X. Bourrat, 1. Structure in Carbons and Carbon Artifacts, in "The Science of Carbon Materials" H. Marsh and F. Rodriguez-Reinoso eds, Universidad de Alicante publisher (June 2000) ISBN 84-7908-544-4

- [3] X. Bourrat, Structure of Pyrocarbons, *World of Carbon, Vol. 3 Fibers and Composites*, P. Delhaes ed. (2003) Ch. 8:159-87, ISBN 0-415-30826-7
- [4] Jean-Marie Vallerot, Xavier Bourrat, Pyrocarbon optical properties in reflected light, *Carbon* 2006;44:1565-71, <http://dx.doi.org/10.1016/j.carbon.2005.12.046>
- [5] P. Dupel, X. Bourrat and R. Paillet, Structure of Pyrocarbon infiltrated by Pulse-CVI, *Carbon* 1995;33(9):1193-204, [http://dx.doi.org/10.1016/0008-6223\(95\)00029-D](http://dx.doi.org/10.1016/0008-6223(95)00029-D)
- [6] S. Goujard, P. Dupel, R. Paillet et X. Bourrat, Method of manufacturing a composite (1995), Societe Europeenne de Propulsion, United States Patent 5,514,453, <http://patft.uspto.gov/netacgi/nph-Parser?patentnumber=5514453>
- [7] X. Bourrat, A.Fillion, R. Naslain, G. Chollon, M. Brendlé, Regenerative laminar pyrocarbon, *Carbon*, 2002;40:2931-2945, [http://dx.doi.org/10.1016/S0008-6223\(02\)00230-0](http://dx.doi.org/10.1016/S0008-6223(02)00230-0)
- [8] X. Bourrat, J. Lavenac, F. Langlais and R. Naslain, The role of pentagons in the-growth of laminar pyrocarbon, *Carbon* 2001;39:2376-80, [http://dx.doi.org/10.1016/S0008-6223\(01\)00223-8](http://dx.doi.org/10.1016/S0008-6223(01)00223-8)
- [9] X. Bourrat, B. Trouvat, G. Limousin, G.L. Vignoles and F. Doux, Pyrocarbon anisotropy as measured by electron diffraction and polarized light, *J. Material Research*, 15(2000) 1
- [10] Ergun S, Yasinsky JB, Townsend JR. Tansverse and longitudinal properties of graphite. *Carbon* 1967;5:403-8.
- [11] Greenaway DL, Harbeke G, Bassani F, Tosatti E. Anisotropy of the optical constants and the band structure of graphite. *Phys Rev* 1969;178(3):1340-8.
- [12] P. Dupel, X. Bourrat and R. Paillet, Structure of Pyrocarbon infiltrated by Pulse-CVI, *Carbon* 1995;33(9):1193-204 [http://dx.doi.org/10.1016/0008-6223\(95\)00029-D](http://dx.doi.org/10.1016/0008-6223(95)00029-D)
- [13] Jean-Marie Vallerot, Xavier Bourrat, Pyrocarbon optical properties in reflected light *Carbon* 44 (2006)1565-71 <http://dx.doi.org/10.1016/j.carbon.2005.12.046>
- [14] F Tuinstra, J Koenig. *The Journal of Chemical Physics* 33 (3) (1970) 1126
- [15] Jawhari T, Roid A, Casado, *Carbon* 1995;33(11):1561-5.
- [16] C Thomsen, S Reich. *Physical Review B* 59 (10) (1999) 6585
- [17] R Saito, A Jorio, AG Souza-Filho, A Grueneis, MA Pimenta, G Dresselhaus, MS Dresselhaus. *Physica B* 323 (1-4) (2002) 100
- [18] R Saito, A Jorio, AG Souza-Filho, G Dresselhaus, MS Dresselhaus, MA Pimenta. *Physical Review letters* 88 (2) (1999)
- [19] Jean-Marie Vallerot, Xavier Bourrat, Arnaud Mouchon, Georges Chollon, *Carbon*, 2006 ; 44 : 1833-44, <http://dx.doi.org/10.1016/j.carbon.2005.12.029>
- [20] J.N. Rouzaud, A. Oberlin, C. Beny-Bassez, Carbon films: Structure and microtexture (optical and electron microscopy, Raman spectroscopy). *THIN SOL. FILMS*. Vol. 105, no. 1, pp. 75-96. 1983
- [21] H. Le Poche, X. Bourrat, M.A. Dourges, G.L. Vignoles, F. Langlais, Influence of the gas phase maturation on the CVD/CVI process and the micro-texture of laminar pyrocarbon from propane, *Proceed. of the 5th Int. Conf. on High Temperature Ceramic Matrix Composites (HT-CMC 5)*, M. Singh et al., eds, 2004 : 81-6, ACS, Westerville OH

- [22] F. Lamouroux, X. Bourrat, R. Naslain and J. Sevely Structure/oxidation relationship in the carbonaceous constituents of 2D-C /PyC / SiC composites Carbon 1993;31(8):1273-88 [http://dx.doi.org/10.1016/0008-6223\(93\)90086-P](http://dx.doi.org/10.1016/0008-6223(93)90086-P)
- [23] X. Bourrat and B. Trouvat, Interface in Ceramic and Carbon Matrix Composites, NATO Advanced Study Institute May 9 to 21, 1998, Antalya, Turkey 3.9, Processing of Ceramics Matrix Composites by Pulse-CVI and Related Techniques
- [24] R. Pailler, H. Lemaire, X. Bourrat, J. Lamon, Interphase in carbon/carbon composite materials, *Proceed. of the 5th Int. Conf. on High Temperature Ceramic Matrix Composites (HT-CMC 5)*, M. Singh et al., eds, 2004, ACS, Westerville OH
- [25] S. Bertrand, C. Droillard, R. Pailler, X. Bourrat and R. Naslain, TEM structure of (PyC/SiC)_n multilayered interphases in SiC/SiC composites, *J. European Ceramic Society* 2000 ;20(1)1-13 [http://dx.doi.org/10.1016/S0955-2219\(99\)00086-2](http://dx.doi.org/10.1016/S0955-2219(99)00086-2)
- [26] S. Labruquère, X. Bourrat, R. Pailler and R. Naslain, Structure and oxidation of carbon/carbon composite : role of the interface, *Carbon* 2001;39:971-984 [http://dx.doi.org/10.1016/S0008-6223\(00\)00142-1](http://dx.doi.org/10.1016/S0008-6223(00)00142-1)
- [27] X. Bourrat, Pyrolytic carbon and their characterization in HTR reactor (Invited Lecture), High Temperature Nuclear Reactor/ECS 2002, 4 to 8 novembre 2002, Cadarache
https://odin.jrc.nl/htr-tn/HTR-Eurocourse-2002/Bourrat_570.pdf
https://odin.jrc.nl/htr-tn/HTR-Eurocourse-2002/Bourrat_571.pdf
- [28] X. Bourrat, O. Dugne Pyrocarbon-based multilayer for HTR fuel particles (Invited Key Note lecture), *Proceed. on CD of Carbon'04, International Conf. on Carbon, Providence RI (USA) 11-16 July 2004*, Am. Carbon Soc. Edt, Omnipress publisher.
- [29] D. Helary, X. Bourrat, O. Dugne, G. Maveyraud, M. Perez., Microstructures of Silicon Carbide and Pyrocarbon Coatings for Fuel Particles for High Temperature Reactors (HTR) *Proceed. of the HTR 2004 in Beijing*
http://www.iaea.org/inis/aws/htgr/fulltext/htr2004_b07.pdf
- [30] D. Hélarly, Xavier Bourrat, O. Dugne, G. Maveyraud, F. Charollais, M. Pérez, F. Cellier [Characterization of Silicon Carbide and Pyrocarbon Coatings for Fuel Particles for High Temperature Reactors \(HTR\)](#) , Workshop on Advanced Reactors With Innovative Fuels, Hosted by Oak Ridge National Laboratory under the auspices of the NEA Nuclear Science Committee, 16-18 February 2005 - Pollard Auditorium, Oak Ridge, Tennessee, USA
<http://www.nea.fr/html/science/meetings/ARWIF2004/3.01.pdf>